

Gamma-ray diffraction – A powerful tool in crystal physics

D. B. Sirdeshmukh

Physics Department, Kakatiya University, Warangal 506 009, India

In recent times, gamma-ray diffraction has emerged as a powerful tool in structural and defect studies of crystals. Though similar in principle to X-ray and neutron diffraction, the very short wavelength of γ -rays gives gamma-ray diffraction an edge over the other diffraction techniques. Experimental details and several applications are discussed.

THE discovery of X-ray diffraction (XRD) by Laue in 1912 opened up two branches in physics, viz. X-ray spectroscopy and X-ray crystallography. Tremendous strides were made in both these branches in the decades that followed. Neutron diffraction (ND) which was discovered in 1936 also developed as a complementary technique in structural studies. Important aspects of XRD and ND are discussed by Bacon¹.

Gamma-ray diffraction (GRD) was demonstrated by Andrade and Rutherford (see ref. 2) in 1914. However, unlike XRD, the application of GRD remained confined to the measurement of γ -ray wavelengths³ for quite some time and it was only in the seventies that GRD emerged as a powerful tool in crystal physics and has been used to advantage for tackling several problems for which the other diffraction techniques were not so effective.

The purpose of this article is to discuss (i) the principle and special features of GRD *vis-à-vis* other diffraction techniques, (ii) the experimental details, and (iii) some typical applications.

Principle and special features

Gamma rays are scattered by electrons associated with the atoms in the crystal and, as such, the principle of GRD is basically the same as that of XRD. GRD is governed by Bragg's law and the expression for the intensity (or reflectivity) of a gamma ray Bragg reflection is the same as that for X-rays⁴. Fourier procedures developed for XRD are applicable to GRD and lead to electron charge distribution.

However, there are some significant differences between XRD and GRD and some special features associated with GRD mainly due to the very short wavelength of γ -rays; these are discussed below⁵⁻¹⁰.

i) The short wavelength of γ -rays results in negligibly

small absorption. This makes the absorption correction to intensities very small and insignificant.

- ii) Another consequence of the low absorption is that thick crystal samples can be used without surface preparation and, further, the presence of ovens, cryostats and pressure devices does not introduce any experimental complications.
- iii) The short wavelength makes extinction effects negligible and if at all a small extinction effect is present, it can be corrected in a comparatively simple manner.
- iv) The energy of γ -rays being much larger than the binding energy of the inner electrons, anomalous dispersion cannot take place and the corresponding anomalous dispersion correction becomes unnecessary.
- v) As will be explained in detail later, because of the short wavelength, the width of the GRD rocking curve is determined only by lattice tilt (mosaicity) and the strain contribution vanishes.
- vi) Though γ -ray sources emit several radiations, each γ -ray line is monoenergetic. Each wavelength can be selected by means of a single channel analyser. Hence, monochromators are not required.
- vii) With the availability of intrinsic Ge detectors for measurement of GRD intensities, the peak-to-background ratio is very high, obviating the need for background subtraction which is a major source of error in XRD.
- viii) γ -ray sources follow the well-known radioactive decay law and consequently there are no random fluctuations in the intensity.
- ix) By measuring transmitted and diffracted intensities, absolute structure factors are determined. As mentioned above, a number of corrections which are unavoidable in processing XRD data do not occur in GRD and, hence, the determination of absolute structure factors can be done with a high degree of accuracy ($\sim 0.5\%$). The accuracy is often limited by non-diffraction factors like limits of error in counting statistics or error in measurement of crystal thickness. Such accuracy is not possible with XRD.
- x) For the sake of completeness, two problems arising out of the short wavelength of γ -rays may be mentioned. Firstly, the entire diffraction pattern is

shifted to very small Bragg angles. Secondly, the short wavelength gives rise to the phenomenon of multiple Bragg scattering which results in a systematic error not present in XRD. However, this undesirable effect is negligible up to $[\sin \theta/\lambda] \leq 0.8$ but for larger values of $[\sin \theta/\lambda]$, a correction becomes necessary.

Experimental details

The main components of a γ -ray diffractometer are the source, the collimators, the goniometer and the detectors.

Several radioactive sources have been tried like ^{198}Au , ^{192}Ir , ^{169}Yb , ^{160}Tb , ^{153}Sm and ^{137}Cs . The relevant properties of some sources are summarized in Table 1. The criteria for the choice of optimum source are specific activity, neutron and γ -ray self-shielding, source half-life and wavelength (energy) of the radiation. Because of their short half-lives, the ^{198}Au and ^{153}Sm sources need repeated irradiation by thermal neutron flux and hence diffractometers employing these sources have to be installed very close to nuclear reactor stations. In contrast, with the ^{192}Ir and ^{137}Cs sources, which have larger half-lives, it is possible to install γ -ray diffractometers even in laboratories away from nuclear reactors.

Schneider¹¹ has discussed the design of the γ -ray diffractometer in use at the Laue-Langevin Institute at Grenoble in France. The plan of this diffractometer is shown in Figure 1a; the design of the goniometer (Figure 1b) and source holder (Figure 1c) are also shown. This instrument uses an irradiated gold foil as the source. In the diffractometer set up at the Hahn-Meitner Institute at Berlin (Schneider)¹², there is provision for using either a gold source or an Ir source.

γ -ray wavelengths are 10 to 50 times smaller than X-ray wavelengths. The result is that whereas in XRD, measurable Bragg reflections occur in the angular range of 3° – 89° , in GRD, the Bragg reflections occur at very small angles in the range $5'$ – 5° . Thus, the GRD experiment is essentially a small angle scattering experiment. Hence, collimation of high degree and an extremely

small beam divergence become necessary. This is achieved by long source-to-sample and sample-to-detector distances (of the order of several meters) and use of thick lead blocks as collimators. The beam cross-section is typically of the order of $0.2 \times 5 \text{ mm}^2$ and beam divergence is in the range $5'$ – $10'$.

The goniometer is of conventional design but with a provision for holding comparatively large crystals. In structure factor measurements, crystals with linear dimensions 3–8 mm are employed and in mosaicity studies, the linear dimensions of crystals used are as large as 1–8 cm. In the latter case, the goniometer has the provision for translating the sample horizontally and vertically to facilitate scanning of different volume elements. In view of the extremely narrow range of Bragg angles, the rotation of the goniometer has to be through still smaller angular ranges. A combination of SLO-SYN step motor and digital electronics ensures rotation in steps of $2''$ (and sometimes even $0.2''$) around the vertical axis. Similar precision is needed in the setting and movement of the detector.

Generally, a NaI(Tl) scintillation detector is used for measuring the intensity of the directly transmitted beam and an intrinsic Ge detector for the measurement of the Bragg reflection intensity; as mentioned earlier, the latter provides a high signal-to-noise ratio eliminating the need for background correction.

Alkire and Yelon¹³ have discussed the design of the γ -ray diffractometer set up at the University of Missouri Research Reactor. Hailed as a 'facility (that) marks the beginning of a new era in GRD', this is a fully automated full-circle diffractometer. The main difference between this instrument and the European instruments is the use of a 1000 Ci strong ^{153}Sm source. In view of the very short half-life (Table 1), the source requires frequent irradiation in the reactor. For this reason, a transportable source holder designed for underwater handling of the source material is required and is described by Alkire and Yelon. Because of the short half-life, intensity measurements stretch over several half-lives. The measurements made in different runs need careful normali-

Table 1. Properties of some γ -ray sources used in GRD

Source	Activity	Half-life	Wavelength (\AA)	Wavelength spread ($\Delta\lambda/\lambda$)	Other relevant features
^{198}Au	80 Ci	2.7 days	0.0301	10^{-6}	Very weak absorption; source has to be replaced every week; commonly employed for absolute structure factor measurements; suitable for thick samples/heavy elements
			0.078	10^{-6}	
^{192}Ir	200 Ci	74 days	0.0205	10^{-6}	0.0392 \AA line generally used; presence of four lines makes it useful especially in determination of extinction-free structure factors
			0.0265	10^{-6}	
			0.0392	10^{-6}	
			0.0603	10^{-6}	
^{153}Sm	1000 Ci	46.8 h	0.12	10^{-5}	Suitable for study of thin samples/light elements
^{137}Cs		29.9 yrs	0.020		

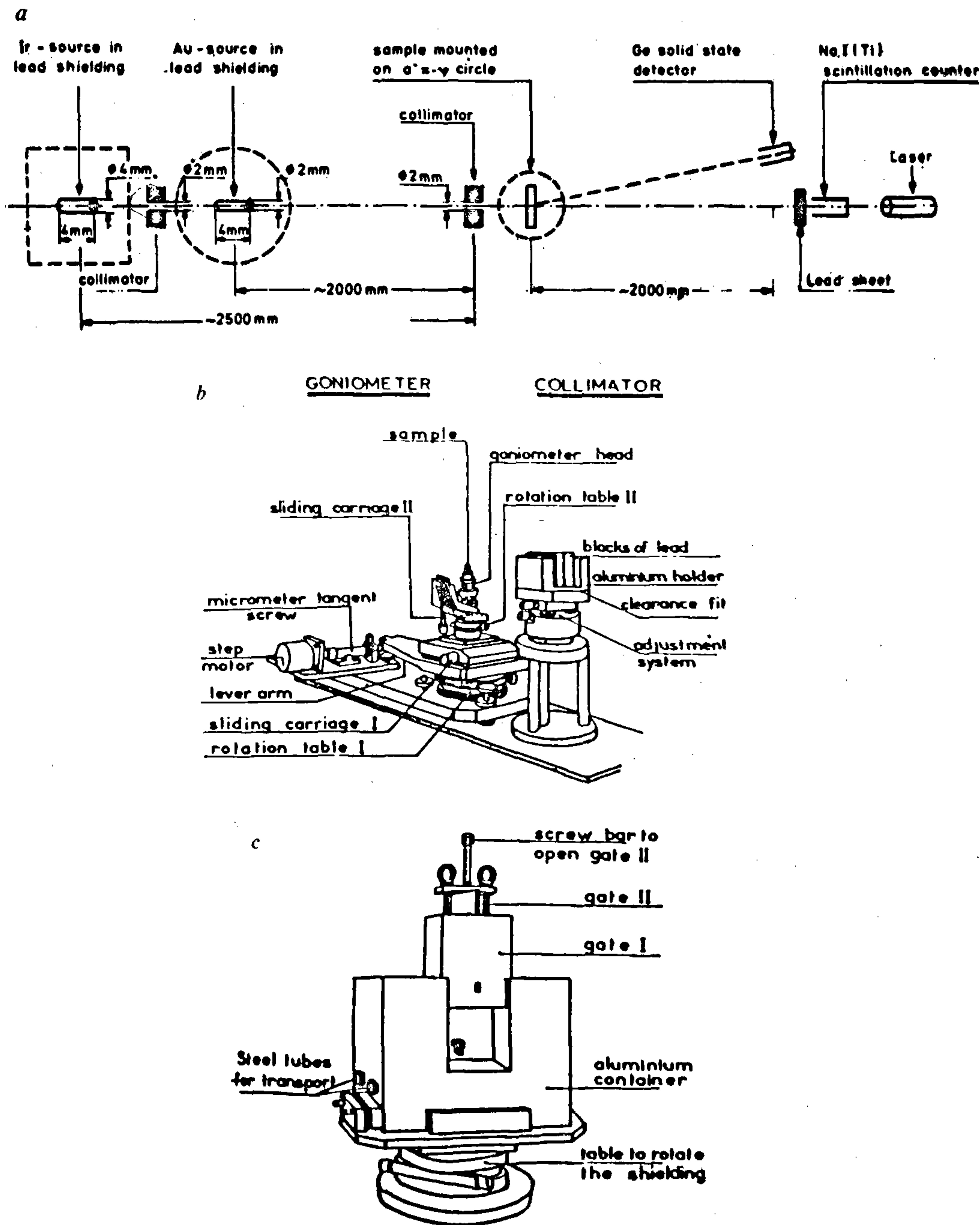


Figure 1. A typical γ -ray diffractometer (refs 11 and 12). *a*, Schematic drawing of the set-up; *b*, Goniometer; *c*, Source holder.

On the other hand, the high strength of the and the consequent intense flux make it ideal lies on light elements and thin samples. The n of the ^{153}Sm source contains several wave- each monochromatic. The availability of several

wavelengths makes it possible to determine extinction-free structure factors. The instrument has a linear drive for the detector with which the sample-to-detector distance can be changed to effect different resolution requirements.

The diffractometers referred above are one-crystal diffractometers; their angular resolution is about $10''$. Schneider¹¹ states that with this angular resolution, fine structure of rocking curves cannot be resolved. Double crystal diffractometers offer a better angular resolution. The first double crystal γ -ray diffractometer was built by Tanner¹⁴ and collaborators at the Rutherford Appleton Laboratory in UK using a ^{198}Au source but has not been put to much use beyond recording the rocking curves for Si crystals.

A double crystal γ -ray diffractometer which uses a ^{192}Ir source has been installed at the Hahn-Meitner Institute; a detailed account of this is given by Schneider and Graf¹⁵. The principle of the double crystal γ -ray diffractometer is shown in Figure 2. As shown, the first crystal is brought into correct diffracting position by displacing the detector at distance $\Delta x^{(1)}$. Similarly, the second crystal (sample) is oriented by displacing the detector by a distance $\Delta x^{(2)}$. The second crystal (sample) is then displaced in the scattering plane perpendicular to the direct beam by a distance Δx which is determined by the Bragg angle of the first crystal and the distance between the two crystals. With Si as the first crystal with distances shown in Figure 2, $\Delta x = 16.34$ mm. The first crystal (Si), though otherwise highly perfect, has internal strains which make its (220) planes have an effective cylindrical curvature about the [111] axis with a radius of curvature of nearly 1000 m. The diffraction of the direct beam at these curved (220) planes results in the diffracted beam being collimated to $1.4''$. The first crystal thus acts like a Soller slit for the second crystal. The resultant angular resolution of such a double crystal set-up is an unprecedented $1''$ and makes the double crystal diffractometer uniquely useful in certain situations; some applications will be discussed later.

Applications of γ -ray diffraction

Absolute structure factors

Using GRD, absolute extinction free structure factors of Be have been determined¹⁹ with an accuracy of 0.5%. By comparison with theoretical model calculations, good agreement was observed with the SCF-HF-LCAO calculations. Similarly the determination of the absolute structure factors of Au by GRD⁷ has made it possible to differentiate between the relativistic and non-relativistic calculations of form factors.

Anisotropy of structure factors

Using GRD, Kretschmer and Schneider¹⁶ could accurately determine the anisotropy of structure factors of vanadium metal. Absolute structure factors were determined and the ratio F_{442}/F_{60k} was determined at temperatures from

70 K to 800 K. The temperature variation of this ratio was found to agree with Willis' model¹⁷.

γ -N synthesis

It is well known that bond distances calculated from the electron charge distribution obtained from XRD are affected by the distortion of the electron cloud by bonding effects. To separate the bonding effect, a difference synthesis is carried out between the structure factors obtained from XRD and ND (the X-N synthesis¹⁸). One limitation in the accuracy of X-N synthesis is that the XRD and ND experiments are carried out on entirely different samples which may have different absorption, extinction and mosaicities. In view of the negligible absorption of γ -rays and neutrons by crystals, it is possible to carry out GRD and ND experiments on the same sample. The results of γ -N synthesis obtained from data on the same sample are superior to the results of the X-N synthesis¹³.

Structural and optical changes in antiferromagnetic crystals

MnF_2 is a classic example of antiferromagnetic ordering; the transition takes place at 67 K. In MnF_2 , the Mn ions are in special positions and the structure can be described in terms of the c/a ratio and the F ion position parameter u .

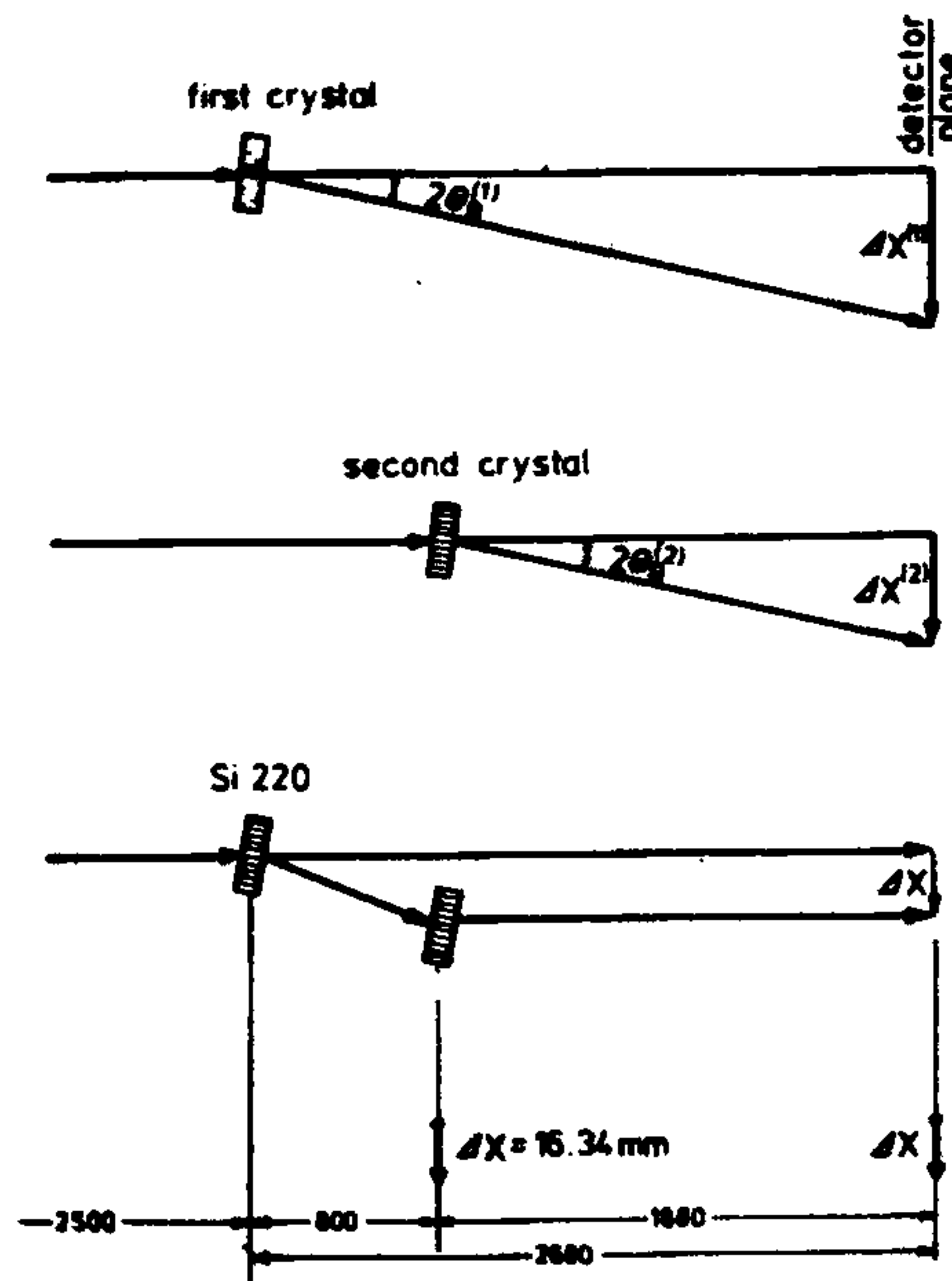


Figure 2. Schematic lay-out of a double crystal γ -ray diffractometer (ref. 14)

At the para-antiferro transition, MnF_2 shows a prominent change in the linear optical birefringence. It was found that the magnetostrictive changes in the lattice constants cannot account for the observed magnetic birefringence. However, it would be possible to account for the birefringence on the basis of the Ewald and Born theory (see ref. 19) in terms of a small (fifth place) magnetostrictive change in the u parameter at low temperatures.

The best X-ray determination²⁰ of the u parameter (Table 2) gave results with fourth place accuracy which was not sufficient to test the Ewald-Born theory results. As mentioned earlier, several corrections required in processing of XRD and ND data become unnecessary in GRD due to which structural parameters can be determined with much greater accuracy. Jauch *et al.*⁸ carried out a GRD determination of u at room temperature and low temperatures with fifth place accuracy. Their results are given in Table 2. The change in u obtained from their results leads to a magnetic birefringence comparable with the observed birefringence. These results have been confirmed by an independent GRD study by Jauch *et al.*²¹ (Table 2). The time-of-flight neutron diffraction technique (TOFND) is capable of yielding structural data with accuracy comparable with GRD, although it does not have the several advantages that arise from the short wavelengths of γ -rays. Jauch *et al.*²¹ determined the u parameter of MnF_2 using the TOFND technique. Their value for u (given in Table 2) at room temperature (RT) is comparable with the GRD value. However, their low temperature (LT) value differs from the GRD value. This is attributed to the noncoincidence of the centroid of the electronic charge distribution (obtained from GRD) and the nuclear positions (obtained from TOFND) in the antiferromagnetic state. As a result the Δu value from TOFND is less than that from GRD.

NiF_2 is another antiferromagnetic crystal isomorphous with MnF_2 . Palmer and Jauch²² carried out exhaustive GRD studies on NiF_2 at RT and LT (in the antiferromagnetic state). Their main results are: (i) there is a magnetostrictive shift in u (Table 2) which is similar

to that in MnF_2 and is consistent with optical birefringence results, (ii) using Stewart's method²³, GRD data is used to obtain the atomic charge density (Figure 3) and (iii) there is excellent agreement between the centroids of atomic charge density obtained from GRD and nuclear positions obtained from ND²⁴.

Mosaicity

Mosaicity is an important aspect of the imperfect state of a crystal and an important factor in determining extinction in a crystal. GRD plays a useful role in the characterization of mosaicity in crystals. The input for such studies is the determination of rocking curves, which are obtained by a step-wise rotation of the crystal through angle ω and recording the counts at every step. The special advantages of GRD in these studies are as follows.

- In a diffraction experiment, the full-width at half maximum (FWHM) of the rocking curve ($\Delta\theta$) contains contributions from the lattice strain ($\Delta\tau/\tau$) as well as mosaicity (η). The relation⁶ is

$$(\Delta\theta)^2 = (\Delta\tau/\tau)^2 \tan^2\theta_B + \eta^2, \quad (1)$$

where θ_B is the Bragg angle. In XRD, the first term is comparable with the second whereas in GRD, because of the very small Bragg angles, the first term is negligible and, thus, the FWHM of the γ -ray rocking curve is almost entirely due to mosaicity. GRD is therefore far superior to XRD as a tool for characterization of mosaicity.

- In order to show dynamical diffraction effects, a defect-free crystal has to have a minimum size. A measure of this size is the extinction length t_{ext} given by^{12,25}

$$t_{\text{ext}} = V/(r_0 F \lambda), \quad (2)$$

where V is the volume of the unit cell, F the structure factor, λ the wavelength and r_0 the classical electron radius. Due to the relative magnitudes of

Table 2. Values of the fluorine position parameter u in MnF_2 and NiF_2 at room temperature and low temperature

Crystal	Method	u			Δu $u(\text{RT}) - u(\text{LT})$
		Room temp.	11 K	15 K	
MnF_2	XRD (ref. 20)	0.3050 (2)			
	GRD (ref. 8)	0.30523 (7)	0.30471 (6)		52×10^{-5}
	GRD (ref. 21)	0.30492 (8)		0.30443 (8)	49×10^{-5}
	ND (ref. 21)	0.30491 (3)		0.30480 (2)	11×10^{-5}
NiF_2	GRD (ref. 22)	0.30364 (9)		0.30326 (8)	38×10^{-5}
	ND (ref. 22)	0.30365 (4)		0.30332 (4)	43×10^{-5}

the wavelengths of X-rays and γ -rays, t_{ext} will be much larger for γ -rays than for X-rays. Thus for a crystal of thickness t_0 , $t_0 \geq t_{ext}$ for X-rays but $t_0 \ll t_{ext}$ for γ -rays. Hence, a crystal which appears perfect when studied with $\lambda = 1.54 \text{ \AA}$ behaves like an imperfect crystal when studied with $\lambda = 0.03 \text{ \AA}$ (ref. 25). Thus certain aspects of mosaic state can be explored only with GRD.

- c) As mentioned earlier, because of the negligible absorption of γ -rays, the mosaicity of large single crystals can be studied without cutting or surface preparation. Figure 4 shows different volume elements of a niobium crystal, the corresponding rocking curves and the variation of the half-width from one volume element to another¹². Although the integrated intensity shows some variation from one volume element to another, the FWHM and, hence, the mosaicity is essentially homogeneous.

As mentioned earlier, the double crystal γ -ray diffractometer is more powerful in giving details of the mosaicity because of the high angular resolution. The following examples are from ref. 15. Figure 5 shows the rocking curves for a Cu crystal obtained with such an instrument; it can be seen that the rocking curves are devoid of any substructure. On the other hand, the rocking curves for a Nb crystal shown in Figure 6 show considerable substructure. It may be noted that this is the same crystal for which a one crystal γ -ray diffractometer has shown rocking curves without any substructure and without much variation (Figure 4). The rocking curves for a synthetic FeS_2 crystal (Figure 7) show a larger substructure for the (111) and than for the (220) reflection planes. This indicates that the crystal growth parallel to (111) lattice planes was perturbed. Figure 8 shows the double crystal rocking curve of a [111] n-type Si wafer. An analysis of the broadened rocking curve indicates a curvature in the (111) planes with a radius of curvature of 460 m.

While the ^{198}Au and ^{192}Ir sources are useful in determining rocking curves of thick samples, only the ^{153}Sm source can handle thin samples. Figure 9 shows the rocking curves of two less than 500 μm thick samples of HgI_2 used as X-ray and γ -ray detectors. These were determined with the help of the Sm based γ -ray diffractometer¹³. It is seen that the mosaic structure of the sample marked grade D is more marked than that of the grade B sample. Also, the efficiency of the grade B sample as a detector was found to be better than that of the grade D sample. Thus, it is possible to link up detector performance with mosaic structure and use GRD in quality-control of radiation detectors.

GRD has been used to characterize the mosaicity of several other crystals like Al, Ge, Be, ice, CaF_2 and gypsum.

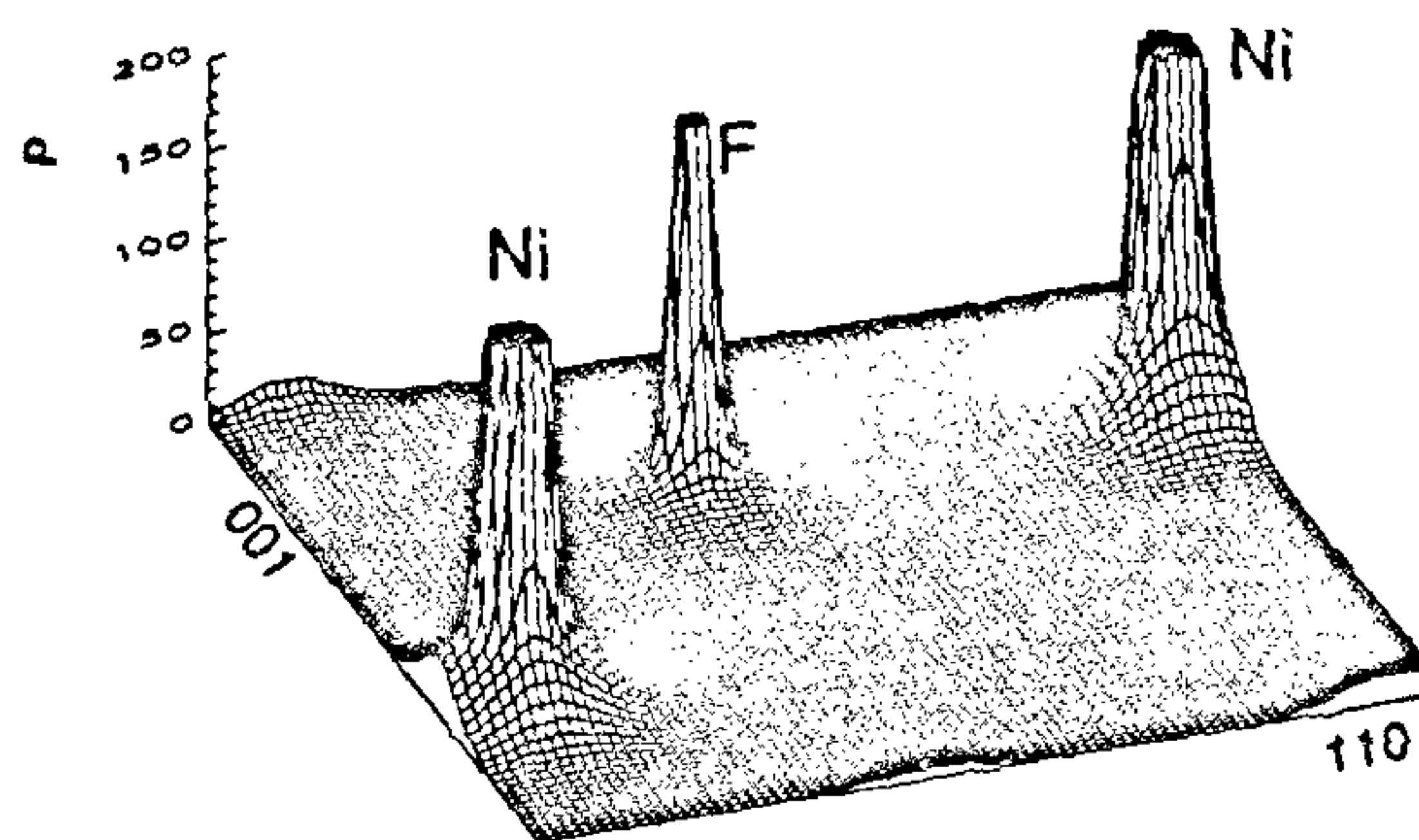


Figure 3. Total charge-density in the (110) plane of NiF_2 at room temperature (ref. 22); ρ in units of $e \text{ \AA}^{-3}$.

Domain structure

The double crystal diffractometer with ^{192}Ir was used by Palmer and Jauch²⁶ to study the domain wall orientation in magnetically ordered NiF_2 which has a Neel temperature of 73 K. GRD experiments were conducted at 15 K. The rocking curves for the (110), (110) and (002) reflections have FWHM of 12", 16" and 22" at RT. At 15 K, the rocking curves for the (110) and (002) reflections broaden (FWHM 38" and 33" respectively) whereas the (110) rocking curve splits into two components (Figure 10). Palmer and Jauch²⁶ have interpreted this observation by proposing a zig-zag domain structure for NiF_2 (Figure 11).

Extinction models

It has been stated earlier that extinction is very much less in GRD than in XRD and the slight amount of extinction, if present, can be corrected in a comparatively simple manner. The ^{192}Ir source emits four wavelengths from 0.0205 to 0.0603 \AA . The Bragg intensities measured at these wavelengths may be extrapolated to $\lambda = 0$ to obtain extinction-free kinematical structure factors irrespective of the nature of the extinction process. On the other hand, by assuming different extinction models, detailed corrections can be applied to these intensities and the models can be tested. Schneider *et al.*²⁷ considered the problem of primary extinction by studying the thickness dependence of the intensity of γ -ray diffracted by Si crystals with thickness between 1 and 3 cm and examined the Darwin model combined with the assumptions of Lorentzian and Gaussian mosaic distributions. They showed that the primary extinction can be accounted for by the sum of two Gaussian distributions. Palmer and Jauch²⁸ determined GRD intensities for a NiF_2

crystal using all the four wavelengths of the ^{192}Ir source. Extinction corrections were applied using different models. By a comparative analysis, it is pointed out that for treating secondary extinction, the Zachariasen⁴ model and the Becker and Coppens' model²⁹ are much better than Sabine's³⁰ model.

Crystal growth studies

The determination of the rate of crystal growth in melt grown crystals is difficult as the liquid-solid interface cannot be observed externally due to the opaqueness of the containers and the surrounding furnace. According

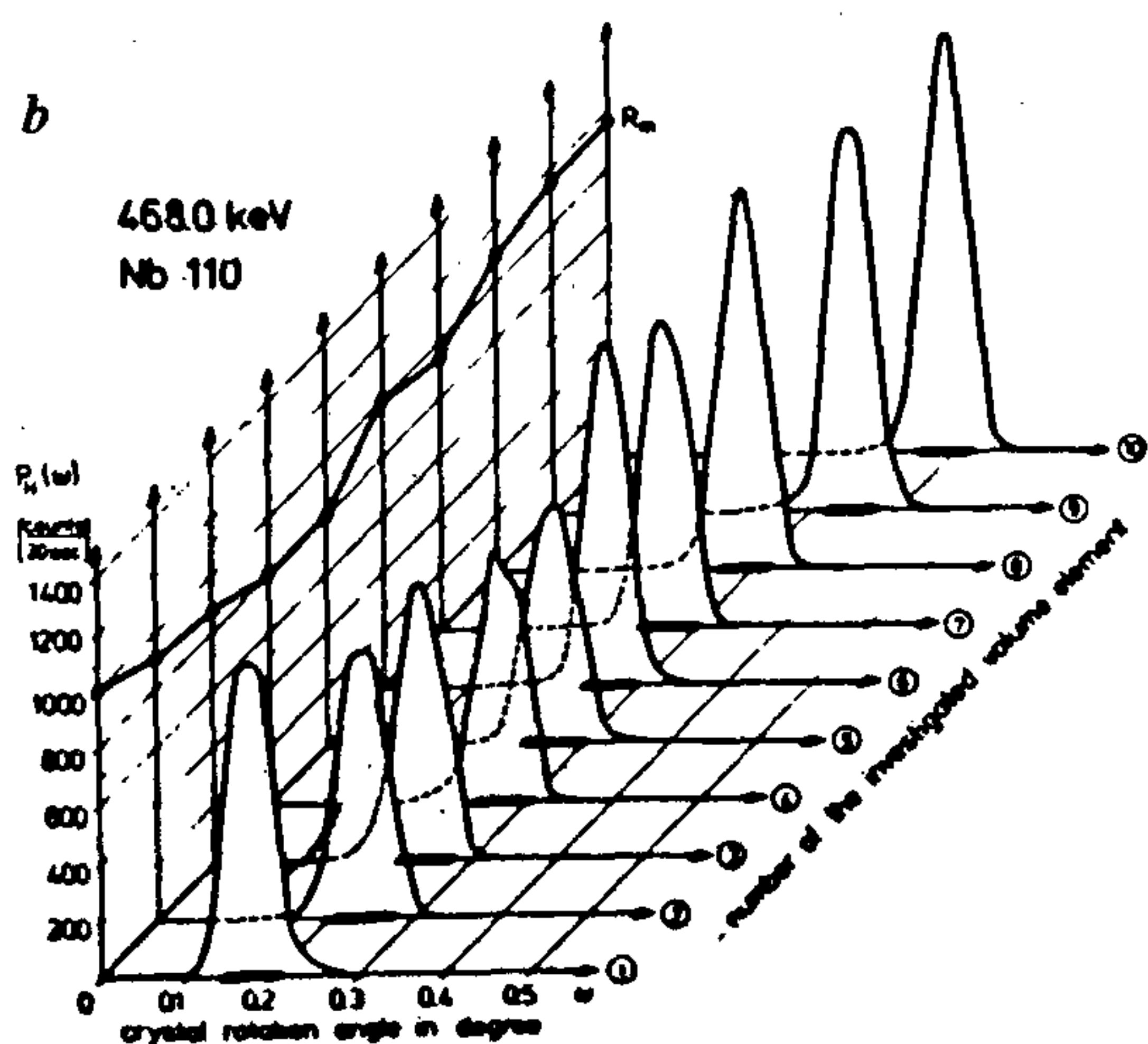
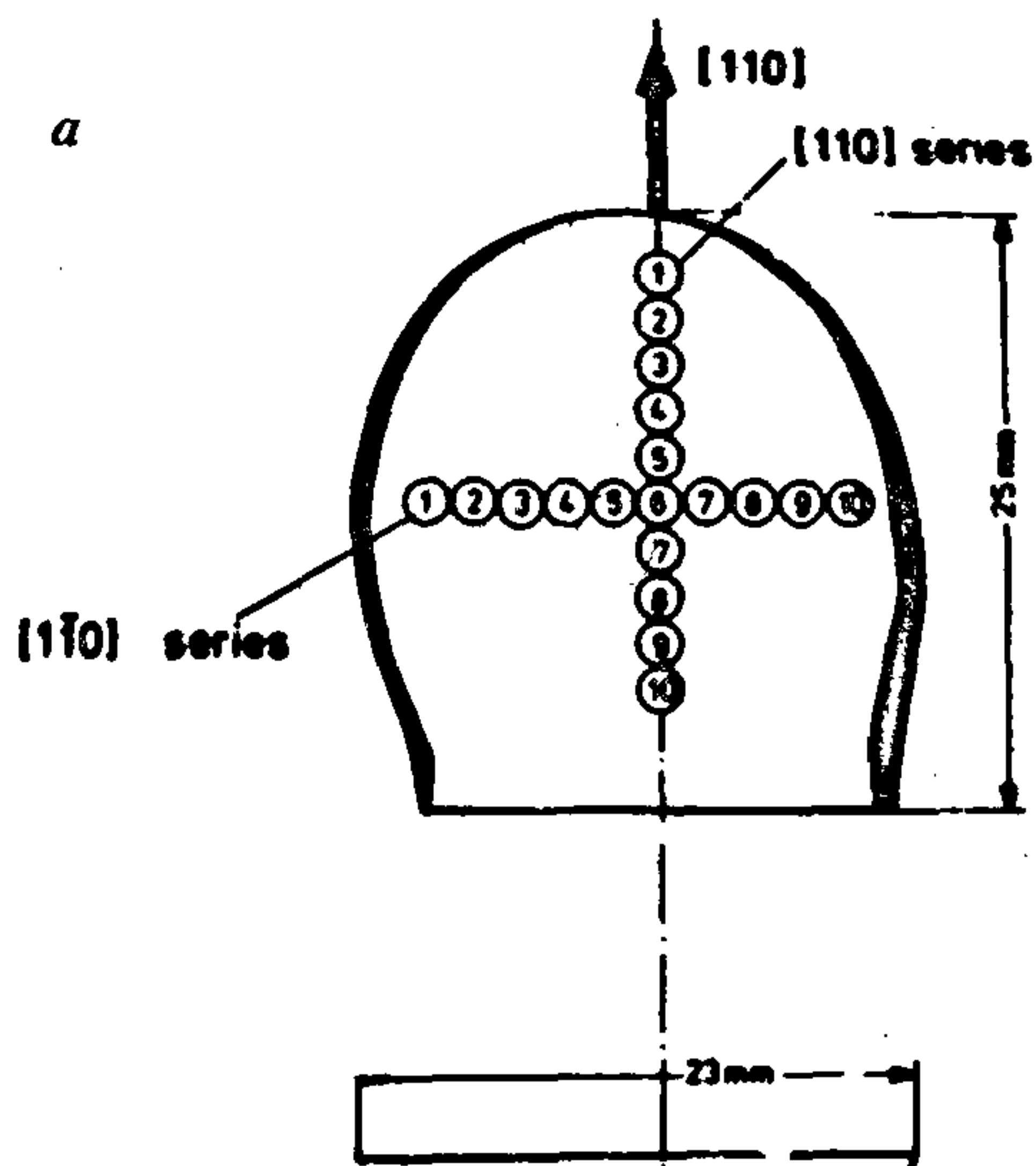


Figure 4. γ -ray rocking curves for a Nb crystal (ref. 12). *a*, Geometry and orientation of the investigated Nb crystal; *b*, Series of rocking curves measured at the (110)₁ reflection of the Nb crystal shown in Figure 4 *a*; $P_{11}(\omega)$ is the Bragg reflected intensity, R_m the integrated intensity and FWHM is shown at the base of each rocking curve.

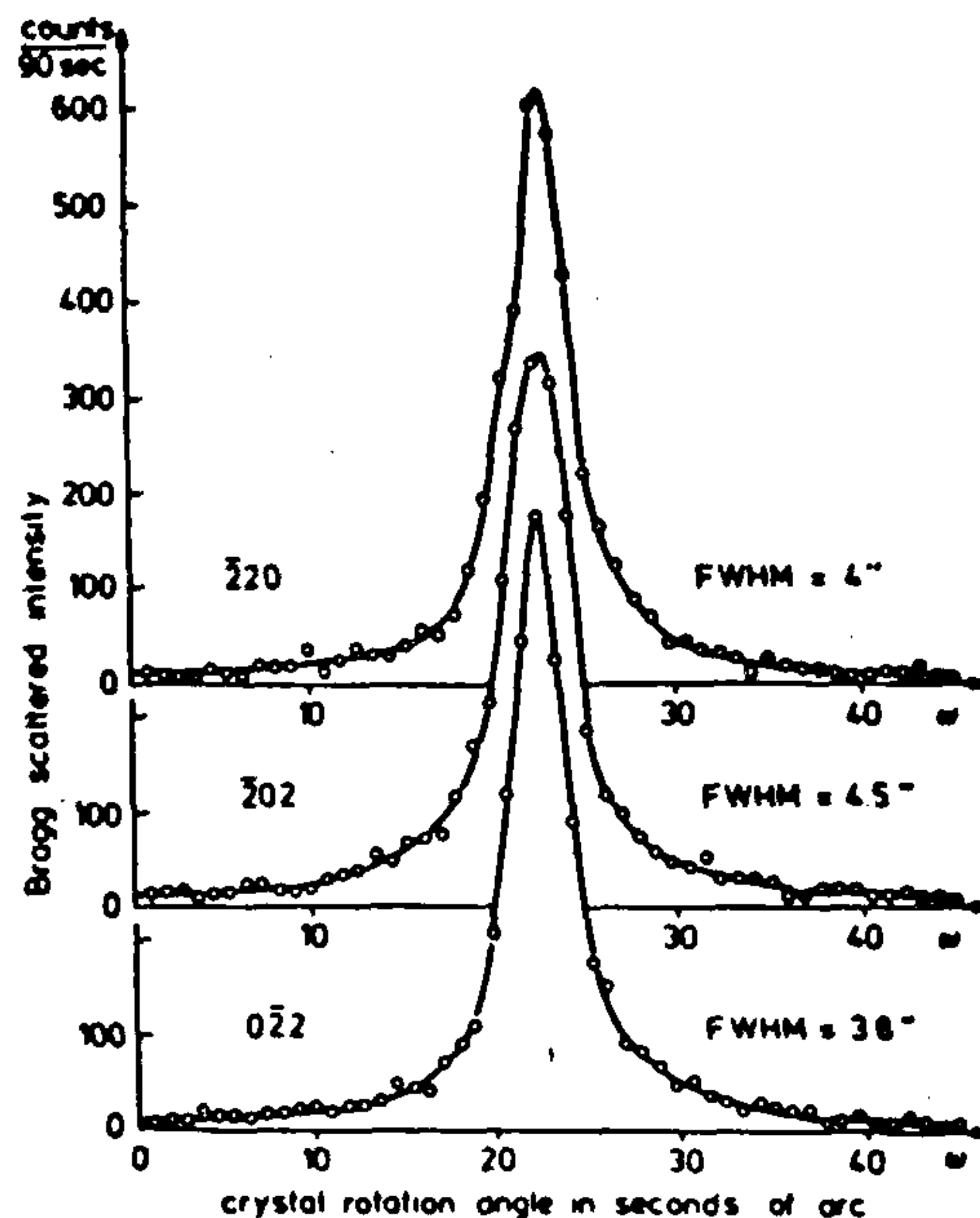


Figure 5. (220) double crystal rocking curves for a Cu single crystal.

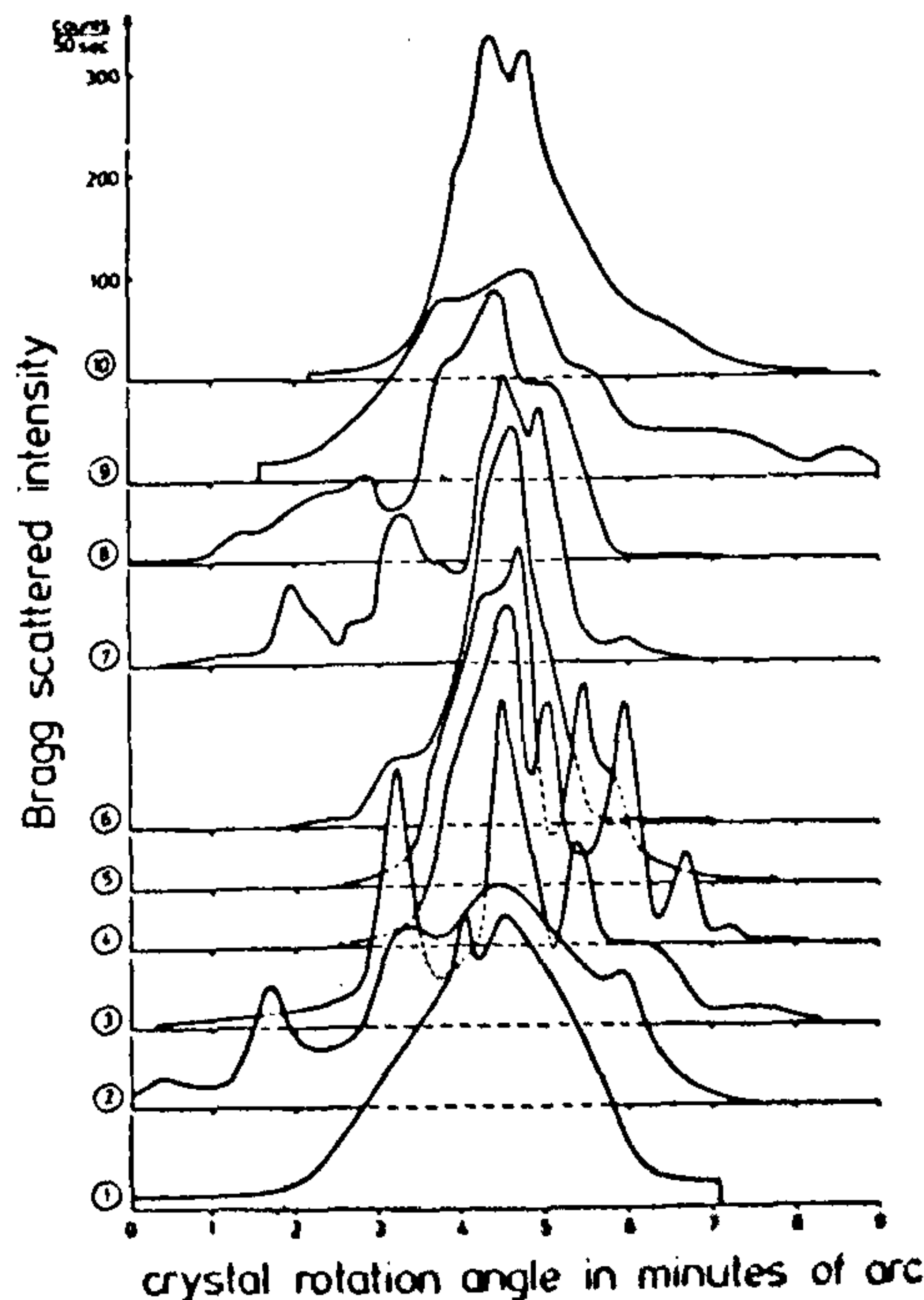


Figure 6. Double crystal rocking curves for the (110) reflection for a Nb crystal (the crystal and the numbering of volume elements are the same as in Figure 4 *a*).

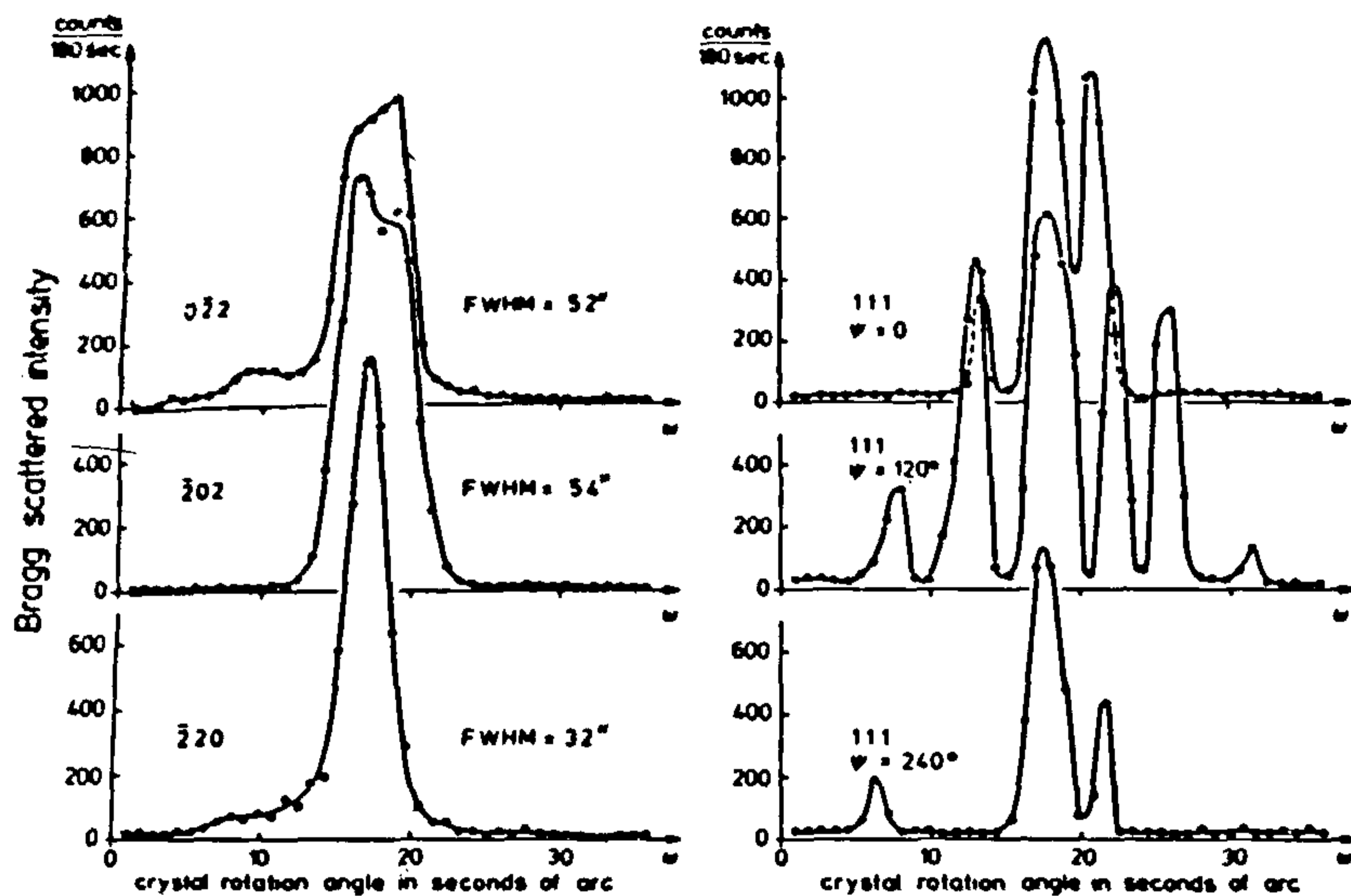


Figure 7. Double crystal rocking curves measured for the (220) and (110) reflections of a vapour grown FeS₂ crystal.

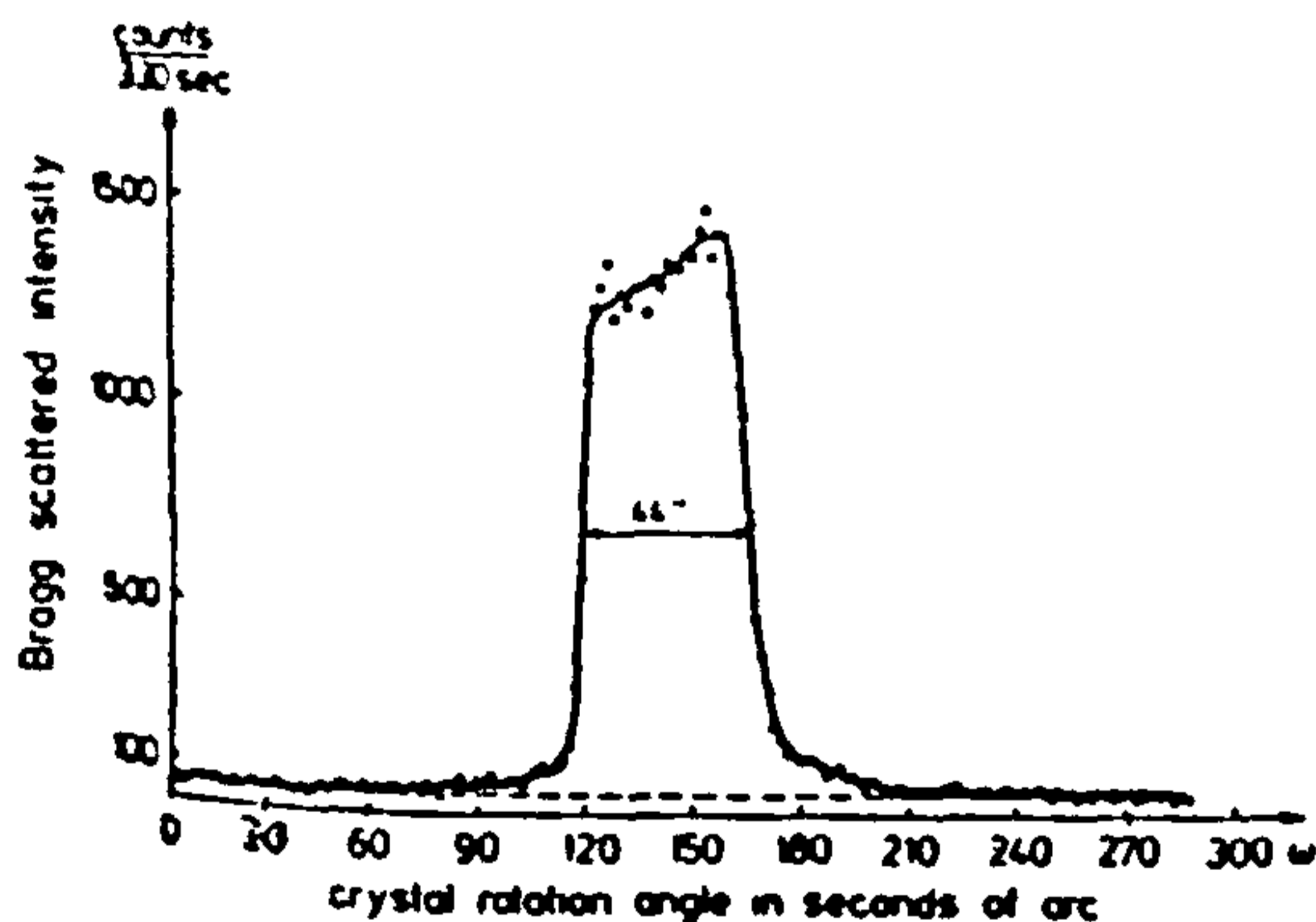


Figure 8. (111) double crystal γ -ray rocking curve of a [111] Si wafer.

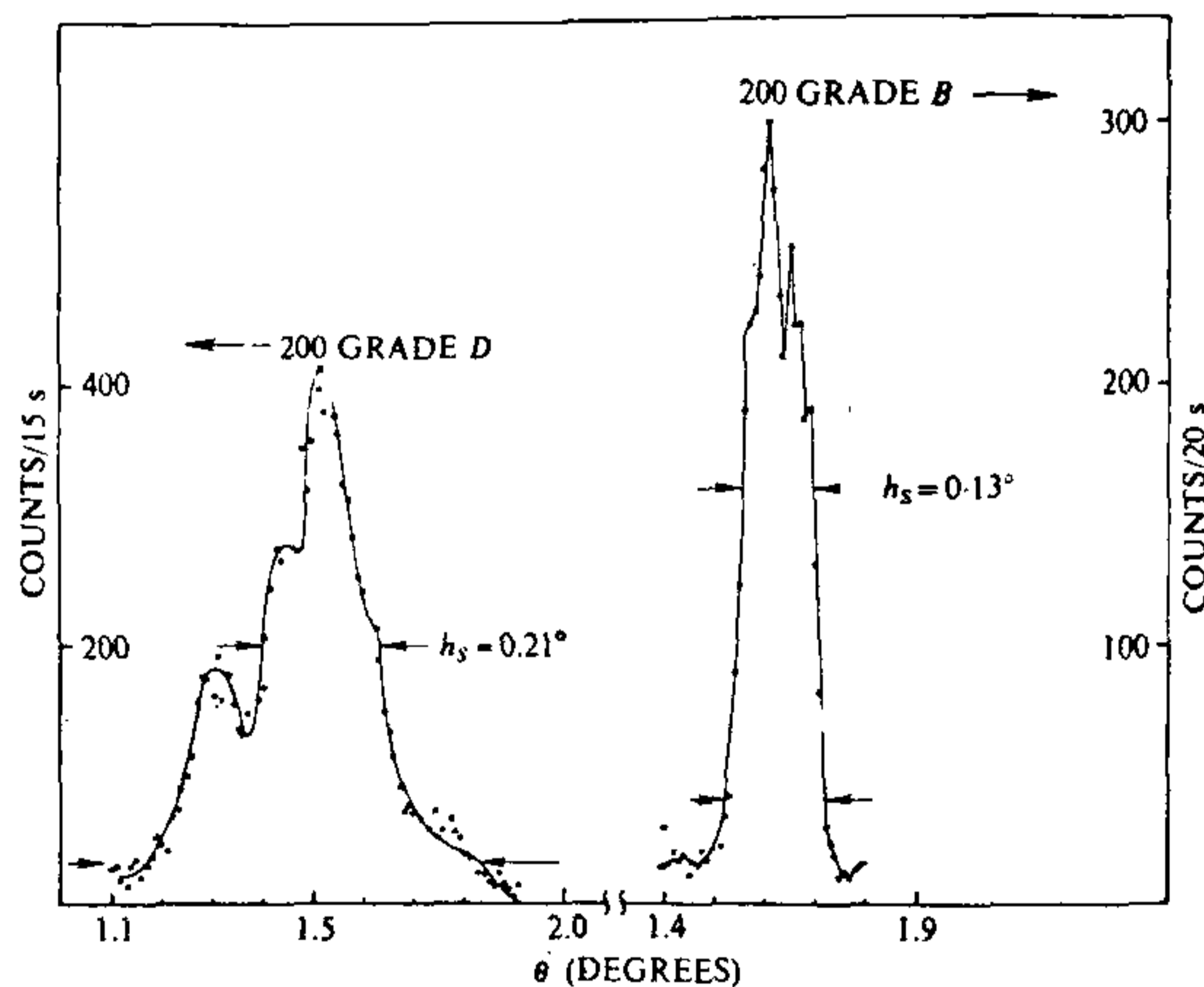


Figure 9. Rocking curves of two thin Hgl₂ crystals cleaved from a single crystal (ref. 13).

to the kinematic theory of diffraction, the integrated intensity is proportional to the diffracting volume. Welter *et al.*³¹ made use of this aspect and the negligible absorption of materials for γ -rays, to determine the rate of growth of a Cu crystal growing in a graphite crucible by means of GRD (Figure 12 a). The intensity of diffraction from the solidified crystal was determined as a function of time (Figure 12 b). As the liquid–solid interface moved up, the intensity increased, finally becoming constant as the interface swept the entire beam; the beam height was 10 mm. In this particular experiment, the growth rate was found to be 2.3×10^{-4} cm/s.

Other applications

GRD has been employed in the study of several other interesting problems like the ferroelectric-to-ferroelastic transition in KDP and RbDP (refs 30, 33), the Jahn-Teller effect in TmSO₄ and TbVO₄ (refs 34, 35), twinning in KDP³⁶ and pressure-induced structural changes in α -NbD_x (ref. 37).

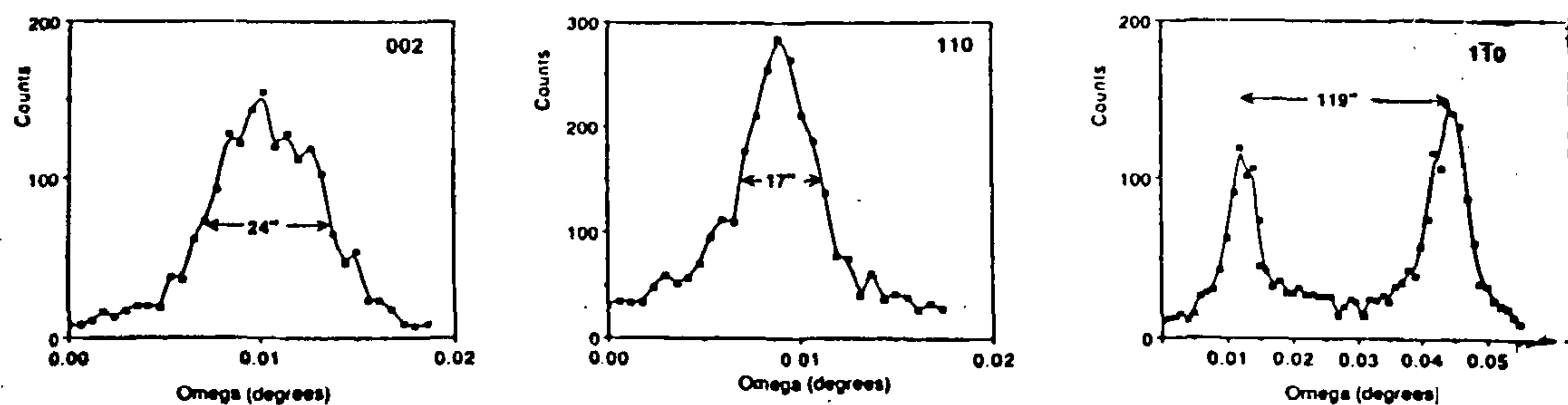


Figure 10. Rocking curves for the (002), (110), (110) reflections of a NiF_2 crystal at 15 K and in the presence of a magnetic field along [100] (ref. 26).

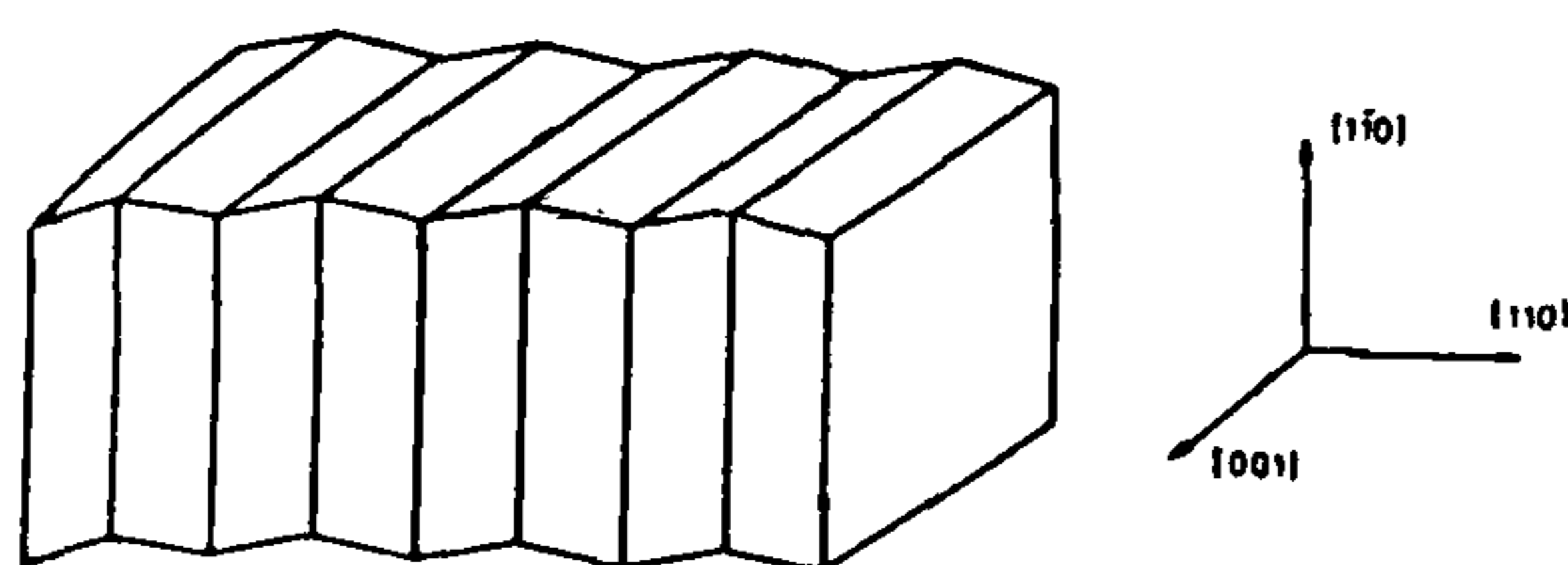


Figure 11. Zig-zag domain structure proposed for the NiF_2 crystal (ref. 26).

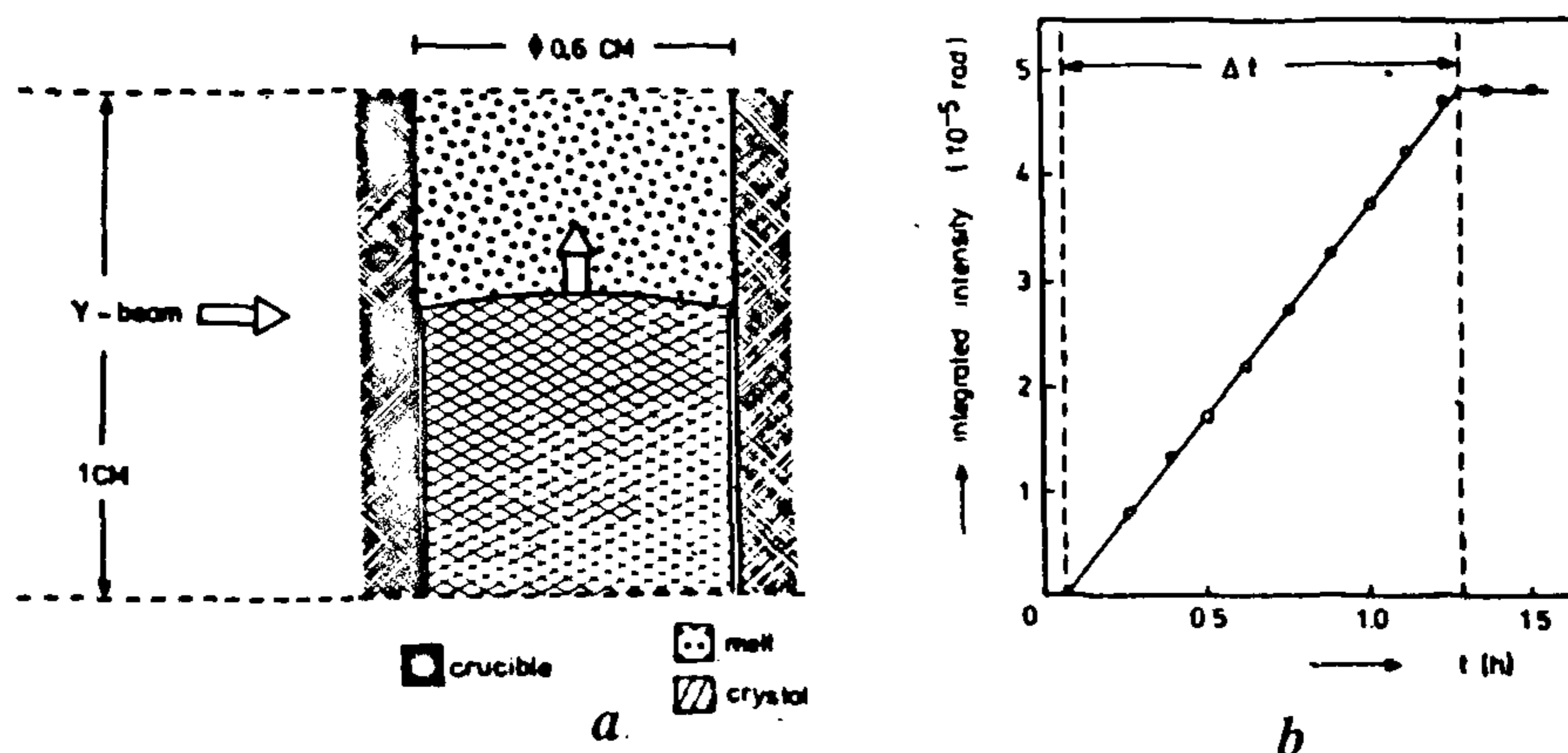


Figure 12. GRD experiment to study crystal growth rate (ref. 31). *a*, Schematic set-up; *b*, Time-dependence of the integrated intensity of the (111) reflection of the growing Cu crystal.

Conclusion

The principles, special features, experimental details and some applications of γ -ray diffraction are discussed. It is shown that the short wavelength bestows on γ -ray diffraction many advantages which do not obtain in X-ray and neutron diffraction, making it a powerful tool in structural and defect studies.

At present, γ -ray diffractometers are available at the Hahn-Meitner Institute at Berlin (Germany), the Laue-

Langevin Institute at Grenoble (France), the Rutherford Appleton Laboratory (UK), the University of Missouri, Columbia (USA) and Kernforschungsanlage Julich (Germany).

More than a dozen laboratories in India have made notable contributions in the field of X-ray crystallography. Defect characterization of crystals by XRD is being carried out at NPL. The contributions of the BARC group in the field of neutron diffraction are internationally recognized. However, GRD facilities are

not available in India. It is hoped that gamma-ray diffraction facility will become available in the near future, in view of its superiority in certain respects over XRD and ND.

1. Bacon, G. E., *X-ray and Neutron Diffraction*, Pergamon Press, London, 1966.
2. Glasstone, S., *Sourcebook on Atomic Energy*, Affiliated East-West Press, New Delhi, 1971.
3. Kaplan, I., *Nuclear Physics*, Addison-Wesley, Massachusetts, 1964.
4. Zachariasen, W. H., *Acta Crystallogr.*, 1967, **23**, 558–564.
5. Schneider, J. R., *J. Appl. Cryst.*, 1976, **9**, 394–402.
6. Freund, F. and Schneider, J. R., *J. Cryst. Growth*, 1972, **13/14**, 247–251.
7. Schneider, J. R., Pattison, P. and Graf, H. A., *Philos. Mag.*, 1978, **38**, 141–154.
8. Jauch, W., Schneider, J. R. and Dachs, H., *Solid State Commun.*, 1983, **48**, 907–909.
9. Hansen, N. K., Schneider, J. R. and Larsen, F. K., *Phys. Rev.*, 1984, **B29**, 917–926.
10. Schneider, J. R., *J. Appl. Cryst.*, 1975, **8**, 530–534.
11. Schneider, J. R., *J. Appl. Cryst.*, 1974, **7**, 541–546.
12. Schneider, J. R., *J. Cryst. Growth*, 1983, **65**, 660–671.
13. Alkire, R. W. and Yelon, W. B., *J. Appl. Cryst.*, 1981, **14**, 362–369.
14. Gani, S. M. A., Clark, G. F. and Tanner, B. K., in *Microscopy of Semiconducting Materials*, Institute of Physics, London, 1981.
15. Schneider, J. R. and Graf, H. A., *J. Cryst. Growth*, 1986, **74**, 191–202.
16. Kretschmer, H. R. and Schneider, J. R., *Solid State Commun.*, 1984, **49**, 971–975.
17. Willis, B. T. M., *Acta Crystallogr.*, 1969, **A25**, 277–289.
18. Coppens, P., in *Neutron Diffraction* (ed. Dachs, H.), Springer, Berlin, 1978.
19. Born, M. and Huang, K., *Dynamical Theory of Crystal Lattices*, Oxford University Press, London, 1968.
20. Alte da Veiga, L. M., Andrade, L. R. and Gonschorek, Z. *Kristallogr.*, 1982, **160**, 171–175.
21. Jauch, W., Schultz, A. J. and Schneider, J. R., *J. Appl. Cryst.*, 1988, **21**, 975–979.
22. Palmer, A. and Jauch, W., *Phys. Rev.*, 1993, **B48**, 10304–10310.
23. Stewart, R. F., *Acta Crystallogr.*, 1976, **A32**, 565–574.
24. Jauch, W., Palmer, A. and Schultz, A. J., quoted in ref. 22.
25. Schneider, J. R., *J. Appl. Cryst.*, 1974, **7**, 547–551.
26. Palmer, A. and Jauch, W., *Solid State Commun.*, 1991, **77**, 95–97.
27. Schneider, J. R., Goncalves, O. D. and Graf, H. A., *Acta Crystallogr.*, 1988, **A44**, 461–467.
28. Palmer, A. and Jauch, W., *Acta Crystallogr.*, 1995, **A51**, 662–667.
29. Becker, P. J. and Coppens, P., *Acta Crystallogr.*, 1974, **A30**, 129–147 and 1975, **A31**, 417–425.
30. Sabine, T. M., in *International Tables for Crystallography*, Kluwer, Dordrecht, 1992.
31. Welter, J. M., Bremer, F. J. and Wenzl, H., *J. Cryst. Growth*, 1983, **63**, 171–173.
32. Bastie, P., Bornarel, J., Lajzerowicz, J., Vallade, M. and Schneider, J. R., *Phys. Rev.*, 1975, **B12**, 5112–5115.
33. Bastie, P., Lajzerowicz, J. and Schneider, J. R., *J. Phys.*, 1978, **C11**, 1203–1216.
34. Mollenback, K., Kjens, J. K. and Smith, S. H., *Electron-Phonon Interactions and Phase Transitions*, Plenum Press, New York, 1977.
35. Smith, S. R. P. and Tanner, B. K., *J. Phys.*, 1978, **C11**, L717–L720.
36. Bastie, P. and Bornarel, J., *J. Phys.*, 1979, **C12**, 1785–1798.
37. Blaschko, O., Klemencic, R., Weinzeirl, P. and Eder, O. J., *J. Phys.*, 1978, **F8**, L149–L151.

ACKNOWLEDGEMENTS. Grateful thanks are due to the referee for a critical reading of the manuscript and for several suggestions which have improved the quality and content of this article. Dr B. J. Rao (TIFR), Prof. K. G. Subhadra and Dr T. Kumara Swamy are acknowledged for much help and cooperation.

Received 4 October 1996; revised accepted 20 March 1997

RESEARCH ARTICLE

Evaluation of water quality index of the river Cauvery and its tributaries

A. Chetana Suvarna and R. K. Somashekar

Department of Botany, Bangalore University, Jnana Bharathi, Bangalore 560 056, India

Water quality of the river Cauvery and its tributaries – Arkavathi and Vrishabhavathi – was assessed by using Bhargava's water quality index. Significant seasonal variation was revealed by the spatially measured physico-chemical characteristics. The water quality index is categorized as class III (satisfactory range) for the Cauvery and Arkavathi rivers and class IV (poor range) for the Vrishabhavathi. The spatial homogeneity of quality was determined by using Duncan's multiple range test.

Southern India, is of great economic importance as apart from being the main source of drinking water, it is utilized for industrial and agricultural purposes. It has been subjected to rapid deterioration over the years due to increasing pollution stress from various sources. Cauvery's sub-tributary Vrishabhavathi receives most of the urban wastes generated in Bangalore City before joining the river Arkavathi, which finally joins Cauvery.

Physico-chemical and biological studies on the river Cauvery have been undertaken¹⁻⁴. However, rivers Arkavathi and Vrishabhavathi have received little attention.

THE Cauvery river system, revered as the Ganges of